

## Use of cavity ring-down spectrometry to quantify $^{13}\text{C}$ -primary productivity in oligotrophic waters

Daffne C. López-Sandoval <sup>1</sup>\* Antonio Delgado-Huertas,<sup>2</sup> Paloma Carrillo-de-Albornoz,<sup>1</sup> Carlos M. Duarte,<sup>1</sup> Susana Agustí <sup>1</sup>

<sup>1</sup>Red Sea Research Center (RSRC), King Abdullah University of Science and Technology (KAUST), Thuwal, Saudi Arabia

<sup>2</sup>Instituto Andaluz de Ciencias de la Tierra, CSIC-UGR, Armilla, Spain

### Abstract

Cavity ring-down spectroscopy (CRDS) is a highly sensitive laser technique that allows the analysis of isotopic signals and absolute concentration of individual molecular species in small-volume samples. Here, we describe a protocol to quantify photosynthetic  $^{13}\text{C}$ -uptake rates of marine phytoplankton by using the CRDS technique ( $^{13}\text{C}$ -CRDS-PP). We validated our method by comparing the  $^{13}\text{C}$ -PP rates measured between CRDS and isotope ratio mass spectrometry (IRMS) in samples with different carbon content (30–160  $\mu\text{gC}$ ). The comparison revealed that  $^{13}\text{C}$ -CRDS-PP rates were highly correlated with those obtained by IRMS (Spearman correlation coefficient,  $\rho = 0.95$ ,  $p < 0.0001$ ,  $n = 15$ ), with a mean difference between the two estimates of  $\pm 0.08 \text{ mgC m}^{-3} \text{ h}^{-1}$ . Moreover, the slope of the relationship between CRDS and IRMS results was not significantly different from 1 ( $F = 0.03$ ,  $p = 0.86$ ), and the intercept did not differ from 0 ( $F = 1.4$ ,  $p = 0.24$ ), indicating that there was no bias in the CRDS relative to the IRMS-based measurements. A separate analysis also showed that despite the difference in volume and carbon content between samples ( $40 \pm 10 \mu\text{gC}$  and  $160 \pm 40 \mu\text{gC}$ , respectively), the  $^{13}\text{C}$ -CRDS-PP technique provides similar results (Mann–Whitney test,  $U = 30.5$ ,  $p = 0.90$ ,  $n = 8$ ). In addition,  $^{13}\text{C}$ -CRDS-PP rates measured along the Red Sea ( $\sim 176 \text{ mgC m}^{-2} \text{ d}^{-1}$ ) agreed with  $^{14}\text{C}$ -based PP rates previously reported for similar locations. Thus, this study evidenced that the  $^{13}\text{C}$ -CRDS-PP method is sensitive enough to quantify carbon fixation rates in oligotrophic regions.

The  $^{14}\text{C}$  method to quantify the photosynthetic activity of marine microalgae ( $^{14}\text{C}$ -PP) was introduced two-thirds of a century ago (Nielsen 1952). Since then, it has been the preferred choice to quantify primary production at sea (Regaudie-de-Gioux et al. 2014) and to calibrate satellite algorithms used to retrieve primary production estimates (Smith et al. 1982; Balch et al. 1989; Behrenfeld and Falkowski 1997). The reasons for the widespread use of this radioisotope tracer approach is due to the relatively simple procedure combined with its high sensitivity to measure carbon uptake rates, even in nutrient depleted marine areas (Ichimura et al. 1962). Currently, concerns about handling radioactive material and its waste products are rising globally, and the number of countries restricting or even prohibiting the use of  $^{14}\text{C}$  in field studies has also increased. Reasons for these limitations are twofold, health and safety concerns together with risks of contaminating

samples aimed to determine the natural abundance of  $^{14}\text{C}$  isotopes on board research vessels. Thus, there is a pressing need to develop new techniques that can match the advantages of the  $^{14}\text{C}$ -PP method but are free of the above concerns.

A decade after the publication of the first  $^{14}\text{C}$ -based primary production studies, Slawyk et al. (1977), using the stable isotope  $^{13}\text{C}$ , introduced an alternative technique to estimate carbon assimilation by mass spectrometry. Though the  $^{13}\text{C}$ -method to measure primary production ( $^{13}\text{C}$ -PP) hinges on the same principle as the  $^{14}\text{C}$ -PP, comparatively few studies have used the  $^{13}\text{C}$ -PP to quantify phytoplankton carbon fixation rates. Earlier findings showed that when simultaneously tested,  $^{13}\text{C}$ -PP measurements tended to be higher than those measured by the  $^{14}\text{C}$ -PP (e.g., Slawyk et al. 1984; Sakamoto et al. 1984; Mousseau et al. 1995). However, differences in incubation volume, filter material, or possibly incomplete combustion of the samples during the spectrometric analysis can explain the discrepancies between protocols (Sakamoto et al. 1984; Slawyk et al. 1984; Mousseau et al. 1995), and once these differences were taken into account, primary production rates measured with the  $^{13}\text{C}$ -PP protocol were in agreement with those obtained by the  $^{14}\text{C}$ -PP method

\*Correspondence: daffne.lopezsandoval@kaust.edu.sa

This is an open access article under the terms of the Creative Commons Attribution-NonCommercial-NoDerivs License, which permits use and distribution in any medium, provided the original work is properly cited, the use is non-commercial and no modifications or adaptations are made.

(López-Sandoval et al. 2018). The primary constraint underpinning the lower use of  $^{13}\text{C}$ -PP is the cumbersome sample preparation. So far, the volumes of sample needed are quite large (1 L or more), and the instruments and training required for isotopic determination (e.g., isotope ratio mass spectrometry, IRMS) are highly specialized and expensive.

The advent of laser absorption spectroscopic techniques to resolve  $^{13}\text{C}$  composition of  $\text{CO}_2$  has generated significant interest across a broad range of applications due to the high-resolution measurements in stable isotope analysis (Berden et al. 2000; Crosson et al. 2002; Crosson 2008). The required instrumentation is more compact, portable, and cost-effective (Berden et al. 2000; Crosson et al. 2002). Moreover, it can be reliably operated on board research vessels to monitor the isotopic signal of stable isotopes (Becker et al. 2012; Bass et al. 2014; Garcias-Bonet and Duarte 2017); therefore becoming a competent alternative to common mass spectrometric analysis (Balslev-Clausen et al. 2013). However, although laser absorption spectroscopic techniques offer compelling benefits, to the best of our knowledge, it has not been used to measure phytoplankton  $^{13}\text{C}$ -primary production rates in the sea. Here, by combining the  $^{13}\text{C}$ -PP method with the advantages of laser spectroscopic measurements, we report a new approximation to measure phytoplankton  $^{13}\text{C}$ -carbon fixation rates by using cavity ring-down spectroscopy (CRDS, i.e.,  $^{13}\text{C}$ -CRDS-PP). Additionally, using relatively small volume samples (500 mL), we demonstrate the applicability of the  $^{13}\text{C}$ -CRDS-PP method to resolve primary production in the oligotrophic Red Sea.

## Materials and procedures

### Sample collection

We collected seawater samples from the Red Sea in November 2016 (winter season), and during the summer of 2017 (June) and 2018 (July and August). Winter sampling was conducted at three different locations along the Saudi Arabian coast (DUST

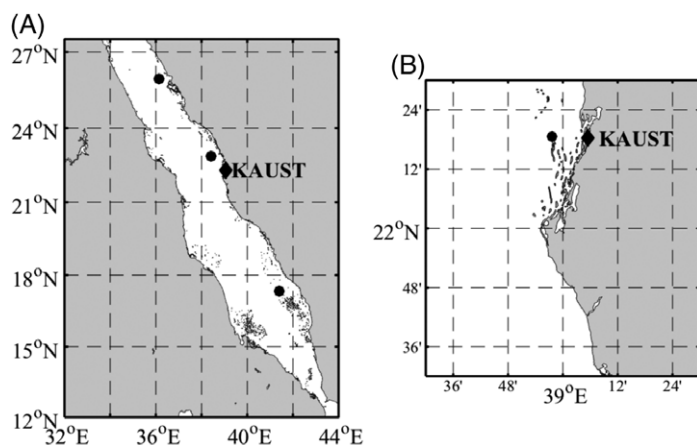


**Fig. 1.** Locations of the sampling sites during (A) the winter period (November 2016) along the Saudi Arabian Red Sea coast and (B) in the summer period at an off-shore station located near Thuwal, Saudi Arabia.

cruise, on board R/V *Thuwal*) (Fig. 1A). Summer samples were taken from a station located off-shore KAUST (Thuwal-Jeddah, Saudi Arabia) (Fig. 1B). During the cruise, water samples from four different optical depths (100–60%, 22%, 8%, and 1% of PAR) were collected with a General Oceanics rosette sampling system fitted with 10-L Niskin bottles between 8:00 and 9:00 am local time. In summer, water was sampled from 2 m to 3 m depth with a Niskin bottle manually deployed around noon.

### Sample processing

For this study, we performed a total of 24 primary production incubations, 12 simulated in situ during the winter cruise (in an on-deck incubator with recirculating surface water), three in situ between summer 2017 and 2018 (in the KAUST harbor) and six under different light conditions in incubation chambers (details below). Water was transferred directly from the Niskin bottles into 10 L acid-washed carboys. The collected water (10 L) was enriched with 50 mL of  $^{13}\text{C}$ -labeled sodium bicarbonate solution (2.18 g of  $\text{NaH}^{13}\text{CO}_3$ , 99.8%  $^{13}\text{C}$ , in 1 L of deionized water) and carefully shaken to homogenize the sample. We distributed the enriched-water into sets of three light and one dark acid-washed polycarbonate bottles (PC) (Fig. 2). We used 2 L PC bottles during the cruise, and both 2 L and 500 mL PC bottles for summer incubations. The final concentration of  $^{13}\text{C}$  in each bottle was  $\approx 153 \mu\text{mol } ^{13}\text{C L}^{-1}$ .

Before the incubation, each set of PC bottles was covered with neutral density mesh to attenuate light intensity according to the corresponding optical depth. At the end of the incubation (3–4 h), the entire bottle content was filtered onto a precombusted Whatman GF/F filter (25 mm diameter for 2 L samples, and 15 mm diameter for 500 mL samples) (Fig. 2). To remove any residual carbonate, we placed the filters in small Petri dishes and remained overnight with 70–100  $\mu\text{L}$  of 50% HCl. After 12–14 h, the filters were frozen at  $-80^\circ\text{C}$ .

Before the analysis, all filters were placed in a desiccator for 24 h. The 25 mm filters were divided into four pieces before each piece was transferred into a tin capsule (all pieces were analyzed). The 15 mm filters were wrapped (whole filter) in large tin capsules (10 mm  $\times$  10 mm size). Then all the samples were loaded into the auto-sampler (attached to the combustion module [CM]). Each sample was analyzed for 600 s. The analysis was done within one month at the Tarek Ahmed Juffali Research in Red Sea Ecology Laboratory (KAUST, Saudi Arabia).

The carbon content and isotopic analysis of primary production samples was done with a CM attached to a CRDS system by Picarro (CM-CRDS G2201-i, Picarro). Dissolved inorganic carbon (DIC) concentration and seawater  $\delta^{13}\text{C}$  of natural samples were measured with the Picarro-CRDS analyser coupled with a Picarro Liaison interface and Picarro AutoMate prep device. The CM-CRDS consists of three components: the CM (elemental analyser), the interface, and the CRDS analyser. The CM (Costech Analytical Technologies) works by the principle of fast sample combustion and conversion to the gases of interest. The samples packed in tin capsules are delivered one by

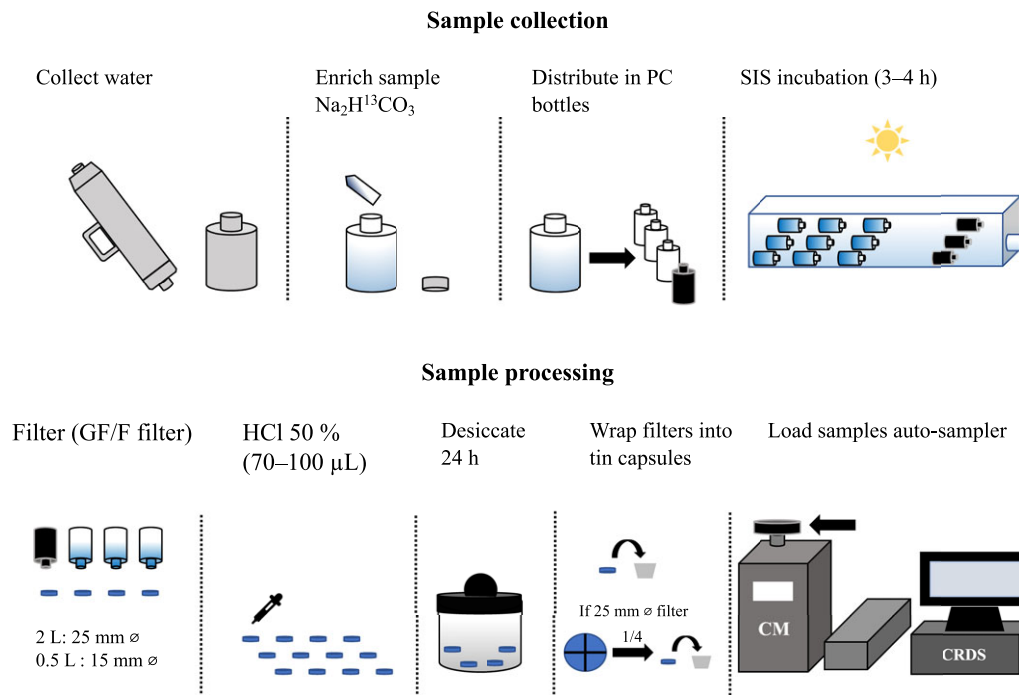


**Fig. 2.** Schematic representation summarizing the different steps to collect and process samples for primary production measurements using the <sup>13</sup>C-CRDS-PP method.

one with an auto-sampler (max. 150 samples) into a combustion quartz tube (prepacked reaction tube, SW, Picarro, CM 61134, OEA Labs) that is surrounded by a furnace controlled at 980°C.

The combustion is achieved through the injection of pure oxygen which reacts with the tin capsule (flash combustion) (Kirsten and Hesselius 1983). As a result, the temperature rises (1700–1800°C) for a few seconds, and the sample is oxidized to a mixture of oxides of carbon and nitrogen that get reduced to N<sub>2</sub>, CO<sub>2</sub>, H<sub>2</sub>O in a copper column at 650°C. The combustion column is packed with chromium oxide (Cr<sub>2</sub>O<sub>3</sub>), and silver cobalt oxide (Ag/Co<sub>3</sub>O<sub>4</sub>) to ensure the conversion of the combustion products. Copper wires in the reduction column adsorb the excess of oxygen not used during the combustion.

The CO<sub>2</sub> produced during the combustion is then carried onwards (N<sub>2</sub> acts as carrier gas) through a water trap of magnesium perchlorate and then both CO<sub>2</sub> and N<sub>2</sub> flow through a short chromatographic column into the caddy interface. The interface handles the CO<sub>2</sub> pulse and splits the carrier gas flow to match the flow rate of the CRDS (Picarro 2009). Subsequently, the gases are pumped into the isotopic analyser to measure the <sup>13</sup>C/<sup>12</sup>C (δ<sup>13</sup>C) ratio. Once the gas is inside the cavity, the instrument compares the ring-down times of an empty cavity (by switching the radiation to wavelengths that are not absorbed by the target molecules) to the ring-down times at wavelengths absorbed by the target gas (CO<sub>2</sub>). The absorbance at each measured wavelength generates an optical spectrum with peaks that correspond to the absorbance by CO<sub>2</sub> (<sup>13</sup>CO<sub>2</sub> or <sup>12</sup>CO<sub>2</sub>) molecules from the sample. The area of a particular peak is proportional to the concentration of <sup>13</sup>C

and <sup>12</sup>C. The ratios between <sup>13</sup>C : <sup>12</sup>C are expressed in delta δ<sup>13</sup>C notation as follows:

$$\delta^{13}\text{C} (\text{‰}) = \left( \left( R_{\text{sample}} / R_{\text{VPDB}} \right) - 1 \right) \times 1000$$

where  $R = {}^{13}\text{C} : {}^{12}\text{C}$  for δ<sup>13</sup>C values in the sample and the international standard, Vienna Pee Dee Belemnite (VPDB). The procedure to calculate phytoplankton photosynthetic rates (<sup>13</sup>C-PP, mgC m<sup>-3</sup> h<sup>-1</sup> measured with the <sup>13</sup>C-CRDS-PP) is based on the isotopic mass balance of <sup>13</sup>C and <sup>12</sup>C of a <sup>13</sup>C-enriched sample at the end of an incubation period ( $t$ , units h). Specifically, we calculated primary production as the isotopic shift of particulate organic carbon (POC) for samples incubated in the light (δ<sup>13</sup>C<sub>POC-light</sub>) relative to those incubated in the dark (i.e., in the absence of photosynthesis, δ<sup>13</sup>C<sub>POC-dark</sub>), and also relative to the isotopic shift of labeled DIC (δ<sup>13</sup>C<sub>DIC-Labeled</sub>) to that in the ambient waters (δ<sup>13</sup>C<sub>DIC-Natural</sub>) per unit of time. Specific uptake rates (h<sup>-1</sup>) were converted to C uptake rates (mgC m<sup>-3</sup> h<sup>-1</sup>) by considering the concentration of POC filtered at the end of the incubation (mgC m<sup>-3</sup>) as shown in Eq. 1:

$${}^{13}\text{C-PP} = \frac{[(\delta^{13}\text{C}_{\text{POC-light}} - \delta^{13}\text{C}_{\text{POC-dark}}) / (\delta^{13}\text{C}_{\text{DIC-Labeled}} - \delta^{13}\text{C}_{\text{DIC-Natural}})] \times \text{POC}}{t} \quad (1)$$

δ<sup>13</sup>C<sub>POC-light</sub> refers to the δ<sup>13</sup>C value at the end of the incubation period, while δ<sup>13</sup>C<sub>POC-dark</sub> corresponds to the δ<sup>13</sup>C value obtained from the dark bottles at the end of the incubation. We estimated that changes of labeled δ<sup>13</sup>C DIC throughout the incubation time due to respiration processes correspond to

≈ 1‰. Thus, the initial and final δ<sup>13</sup>C<sub>DIC</sub> values remain relatively similar (≈ δ<sup>13</sup>C<sub>DIC-Labeled</sub>). δ<sup>13</sup>C<sub>DIC-Natural</sub> refers to the natural values of δ<sup>13</sup>C-DIC (unlabeled water).

δ<sup>13</sup>C<sub>DIC-Labeled</sub> was determined taking into consideration the enrichment of the DIC pool with <sup>13</sup>C as follows:

$$\delta^{13}\text{C}_{\text{DIC-Labeled}} = \left[ \frac{\left( \frac{\mu\text{M}^{13}\text{C}_{\text{DIC-Natural}} + \mu\text{M}^{13}\text{C}_{\text{DIC-stock}}}{\mu\text{M}^{12}\text{C}_{\text{DIC-Natural}} + \mu\text{M}^{12}\text{C}_{\text{DIC-stock}}} \right)}{\frac{^{13}\text{C}}{^{12}\text{C}} \text{V-PDB}} - 1 \right] \times 1000$$

where  $\mu\text{M}^{13}\text{C}_{\text{DIC}} = [\text{DIC}] \times [(\% \text{ Atom } ^{13}\text{C})/100]$  and  $\mu\text{M}^{12}\text{C}_{\text{DIC}} = [\text{DIC}] \times [(100 - \% \text{ Atom } ^{13}\text{C})/100]$ . The % Atom <sup>13</sup>C for the DIC stock is indicated in the commercial label of the NaH<sup>13</sup>CO<sub>3</sub> stock. The <sup>12</sup>C<sub>DIC-Natural</sub> (samples before being labeled) is derived from the δ<sup>13</sup>C values. Seawater has relatively constant δ<sup>13</sup>C<sub>DIC-Natural</sub> values (compared to the high variability associated with the labeled DIC; δ<sup>13</sup>C<sub>DIC-Labeled</sub>). Hence, the variability of δ<sup>13</sup>C<sub>DIC-Natural</sub> is negligible in the calculus of <sup>13</sup>C-PP (i.e., a difference of 1‰ in δ<sup>13</sup>C<sub>DIC-Natural</sub> implies a change in the third decimal of primary production results).

### Standardization of the Picarro-CRDS

We calibrated the Picarro-CRDS using internal and certified VPDB standards from the International Atomic Energy Agency (IAEA) and Reston Stable Isotope Laboratory (United States Geological Survey, USGS) with δ<sup>13</sup>C values within the range of our measurements (~ 450‰, on average). The certified standards from the IAEA were: IAEA-CH-6 (-10.45‰), IAEA-C3 (-24.72‰), and IAEA-303 B (≈ +450‰). USGS standards were: USG62 (-14.79‰), USG40 (-26.39‰), and USG41a (+36.55‰).

### Comparison between <sup>13</sup>C-CRDS-PP and <sup>13</sup>C-PP measurements obtained by IRMS

To validate <sup>13</sup>C-CRDS-PP method, we collected water on a station off-shore KAUST (Fig. 1) on two different occasions. On each day, water was distributed into three different sets of PC bottles, each set consists of six light and two dark PC bottles (24 bottles in total). Water samples were incubated for 3 h in Percival Intellus Ultra C8 incubation chambers (Percival Scientific) at 31°C (same as measured in situ) and each set was incubated under different light conditions (278 ± 13, 296 ± 8, 333 ± 5 μmol m<sup>-2</sup> s<sup>-1</sup>). After the incubation period, samples were processed as described in the sample processing section. From each set, three light and one dark sample were analyzed by CRDS, while the other four samples (3 light and one dark) were analyzed by IRMS at the Stable Isotope Laboratory at the Instituto Andaluz de Ciencias de la Tierra. The IRMS analysis was performed on a Carlo Elba NC1500 (Milan, Italy) elemental analyser coupled on-line via a ConFlow II with Delta Plus XP (Thermo-Finnigan, Bremen, Germany) mass spectrometer (EA, IRMS).

### Additional measurements

In addition to primary production samples, water samples were collected to determine chlorophyll *a* (Chl *a*) and dissolved inorganic nutrient concentrations. For the Chl *a* analysis, 200 mL samples were taken at nine to 10 discrete depths (between 3 m and 200 m) and filtered through Whatman GF/F filters (25 mm diameter). The filters were kept frozen at -20°C until further analysis back on land. Pigments were extracted using 90% acetone and left in the dark at 4°C for 24 h. Chl *a* concentration was estimated with the non-acidification technique using a Turner Design Trilogy Fluorometer, previously calibrated with pure Chl *a*. Concentrations of dissolved inorganic nitrogen (NO<sub>3</sub><sup>-</sup> + NO<sub>2</sub><sup>-</sup>) and phosphorous (PO<sub>4</sub><sup>3-</sup>) were determined with a SEAL AA3 Segmented Flow Analyzer (SEAL Analytical) using standard methods (Hansen and Koroleff 1999). The detection limits were 0.05 μM for nitrate, 0.01 μM for nitrite, and 0.01 μM for phosphate.

### Assessment and discussion

#### CRDS and δ<sup>13</sup>C (CO<sub>2</sub>) calibration

CRDS, also known as cavity ring-down laser absorption spectroscopy, is an ultrasensitive absorption method that measures the optical absorbance of a gas sample introduced into a high-finesse optical cavity (Berden et al. 2000; Crosson et al. 2002). The cavity has an extremely long effective absorption path length (~ 20 km in the CRDS-Picarro) which allows keeping the sample volume relatively small (Berden et al. 2000). This characteristic represents an advantage for primary production measurements, particularly in low-productivity regions of the ocean where phytoplankton biomass is low and obtaining reliable measurements of primary production is particularly challenging. To assess the analytical precision and accuracy of the δ<sup>13</sup>C analysis for samples with low carbon concentration, we performed repeated measurements with solutions of a wide carbon concentration range (10 μgC to 1 mgC). Solutions were prepared with internal standards provided by the Instituto Andaluz de Ciencias de la Tierra-CSIC, Spain. The analytical precision (determined as the standard error of the mean from 47 replicated samples) was ± 0.13‰, while the accuracy (defined as the difference between theoretical δ<sup>13</sup>C values and δ<sup>13</sup>C measured from internal standards) was ± 0.52‰.

#### Comparison of photosynthetic <sup>13</sup>C-uptake rates by CRDS (<sup>13</sup>C-CRDS-PP) and by IRMS (<sup>13</sup>C-IRMS-PP)

In this test, phytoplankton carbon fixation rates ranged from 0.81 mgC m<sup>-3</sup> h<sup>-1</sup> to 3.64 mgC m<sup>-3</sup> h<sup>-1</sup>, while the POC concentration in the filters ranged from 0.03 mgC to 0.16 mgC. <sup>13</sup>C-CRDS-PP measurements correlated significantly with <sup>13</sup>C-IRMS-PP measurements (Spearman correlation coefficient, ρ = 0.95, *p* < 0.0001, *n* = 15) (Fig. 3), with a mean difference between the two uptake rates of ± 0.08 mgC m<sup>-3</sup> h<sup>-1</sup>. Since the slope of the relationship between <sup>13</sup>C-CRDS-PP and

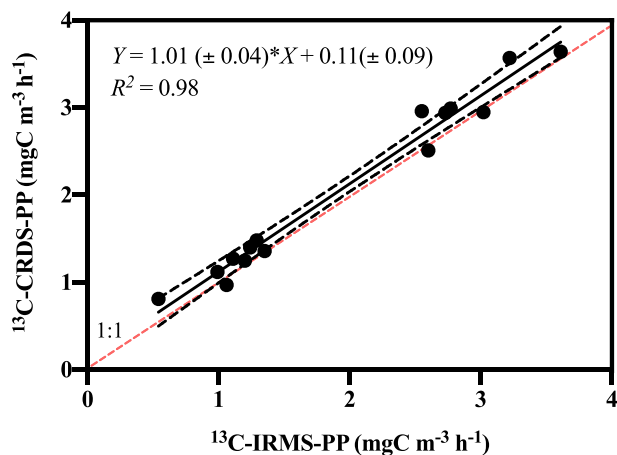


**Fig. 3.** Relationship between carbon fixation rates measured by CRDS (<sup>13</sup>C-CRDS-PP) and by IRMS (<sup>13</sup>C-IRMS-PP). The dashed lines represent the 95% confidence interval (CI = 0.86 to 0.98). The slope and the intercept were not significantly different from 1 ( $F = 0.03$ ,  $p = 0.86$ ) and 0 ( $F = 1.4$ ,  $p = 0.24$ ), respectively. The red dashed line indicates the 1 : 1 relationship.

<sup>13</sup>C-IRMS-PP rates was not significantly different from 1 ( $F = 0.03$ ,  $p = 0.86$ ), and the intercept did not differ from 0 ( $F = 1.4$ ,  $p = 0.24$ ), our results indicates that <sup>13</sup>C-CRDS-PP results are similar to those obtained by IRMS. Taking all the <sup>13</sup>C-uptake measurements included in this study ( $n = 24$ ), we determined that the precision of the <sup>13</sup>C-CRDS-PP measurements was  $\pm 0.04$  mgC m<sup>-3</sup> h<sup>-1</sup>.

#### Measures of isotopic enrichment ( $\delta^{13}\text{C}$ ) and carbon content of samples with different volumes

We measured phytoplankton <sup>13</sup>C-enrichment and the carbon content of samples simultaneously incubated in 500 mL and 2 L. The mean carbon content measured in 500 mL samples was  $0.04 (\pm 0.01)$  mgC, whereas in the 2 L samples was  $0.16 (\pm 0.04)$  mgC. Despite that POC content in the 500 mL samples differed significantly to those measured in the 2 L samples (*U*-Mann-Whitney test,  $p < 0.001$ ,  $n = 8$ ), neither the delta values (Mann-Whitney test,  $U = 31$ ,  $p = 0.96$ ,  $n = 8$ ), nor the carbon fixation rates differed significantly (Mann-Whitney test,  $U = 30.5$ ,  $p = 0.90$ ,  $n = 8$ ). On average,  $\delta^{13}\text{C}$  values in the 500 mL samples were 449‰ [SD, 178], while the average for the 2 L samples was 446‰ [SD, 193]. Mean <sup>13</sup>C-CRDS-PP in the 500-mL samples was  $1.96$  mgC m<sup>-3</sup> h<sup>-1</sup> [SD, 0.74] and the average photosynthetic rates measured in the 2 L samples was  $2.01$  mgC m<sup>-3</sup> h<sup>-1</sup> [SD, 0.8] (Fig. 4).

The standard deviations obtained from the <sup>13</sup>C-CRDS-PP measurements (between the 500 mL and 2 L samples) were higher than analytical error ( $\pm 0.04$  mgC m<sup>-3</sup> h<sup>-1</sup>) associated to the <sup>13</sup>C-CRDS-PP method. Thus, the reported variability could be explained as inherent experimental errors due to small changes in the bottles' conditions between replicates. Therefore, the differences observed in the carbon content between large and small volume incubations (2 L and 500 mL)

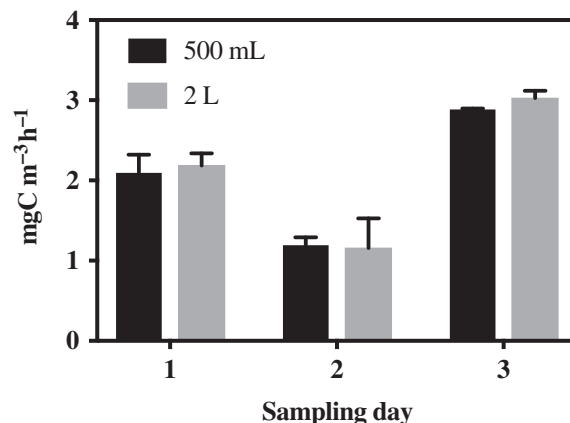


**Fig. 4.** Mean and standard error of primary production measurements obtained from simultaneous incubations of 2 L and 500 mL samples.

did not incur any bias on primary production rates. Our results evidenced that the sensitivity of the CRDS is sufficient to yield robust estimates of <sup>13</sup>C-CRDS-PP with 500 mL samples and a carbon content between  $30 \mu\text{g}$  and  $50 \mu\text{g}$  (i.e.,  $60\text{--}100 \mu\text{g C L}^{-1}$ ).

#### Primary production measurements along the Red Sea

We used the <sup>13</sup>C-CRDS-PP to quantify phytoplankton photosynthetic rates in the Red Sea at three different sites located along a south–north transect. The three selected locations differed in nutrient availability, phytoplankton abundance (Chl *a* concentration), and photosynthetic rates. At the southernmost station (SRS), Chl *a* concentration increased from  $0.78 \mu\text{g Chl } a \text{ L}^{-1}$  in the surface, to  $0.91 \mu\text{g Chl } a \text{ L}^{-1}$  at 21 m (Chl *a* max), then decreasing to  $0.1 \mu\text{g Chl } a \text{ L}^{-1}$  close to limit of the photic zone (Zeu = 1% of PAR  $\approx 60$  m). In this station, dissolved inorganic nitrogen concentration (DIN =  $\text{NO}_2 + \text{NO}_3$ ) increased from  $1.16 \mu\text{M}$  at the surface to  $10.6 \mu\text{M}$  at the Zeu, while phosphate concentration increased from  $0.12 \mu\text{M}$  at the surface to  $0.94 \mu\text{M}$  at the Zeu. At the central (CRS) and the northern station (NRS), Chl *a* concentration throughout the water column decreased relative to the SRS. In these stations, surface Chl *a* ranged from  $0.3 \mu\text{g Chl } a \text{ L}^{-1}$  to  $0.4 \mu\text{g Chl } a \text{ L}^{-1}$ , while at the Chl *a* max (between 75 m and 80 m), the concentration ranged from  $0.5 \mu\text{g Chl } a \text{ L}^{-1}$  to  $0.8 \mu\text{g Chl } a \text{ L}^{-1}$ . Nutrient availability also decreased toward the north of the basin. DIN ranged from  $0.75 \mu\text{M}$  (at the surface) to  $1.9 \mu\text{M}$  (at the Zeu), while phosphate concentration was  $< 0.05 \mu\text{M}$  throughout the water column. The decrease in nutrient availability and Chl *a* toward the northernmost station is consistent with the growing oligotrophic conditions that characterize the North of the Red Sea (Raitsos et al. 2013; Kürten et al. 2016; Zarokanellos et al. 2017).

The vertical distribution of carbon fixation rates was also markedly different between the southern (SRS) and the northern Red Sea (NRS) (Fig. 5). In the NRS, phytoplankton photosynthetic rates remained  $< 0.4$  mgC m<sup>-3</sup> h<sup>-1</sup>, peaking at 30 m and

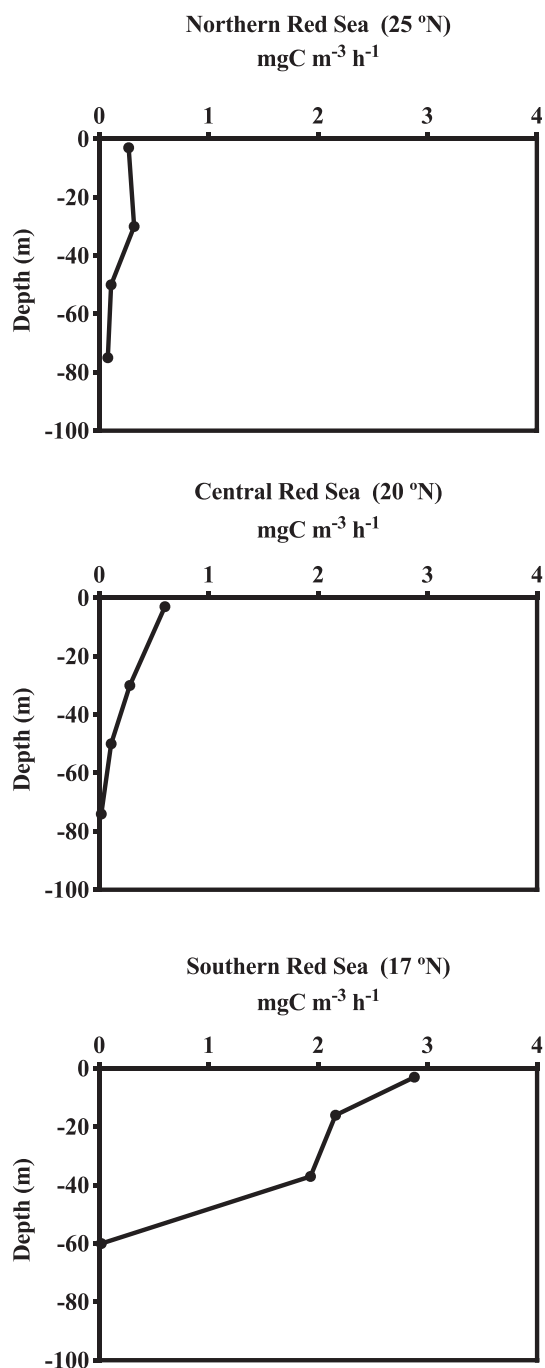


**Fig. 5.** Vertical profiles of primary production measured in the Northern Red Sea (25°N), Central Red Sea (20°N), and Southern Red Sea (17°N) at different optical depths (100–60%, 22%, 8%, and 1% of the photosynthetically active radiation).

then decreasing with depth (Fig. 5A). In the SRC, carbon fixation rates ranged between 2  $\text{mgC m}^{-3} \text{h}^{-1}$  and 3  $\text{mgC m}^{-3} \text{h}^{-1}$  in the first 40 m, then decreasing toward the limit of the photic layer (Fig. 5C). Except for the SRS station, where depth-integrated primary production rate was  $98 \pm 4.3 \text{ mgC m}^{-2} \text{h}^{-1}$  ( $\sim 1.01 \text{ gC m}^{-2} \text{d}^{-1}$ ), low photosynthetic rates characterized the

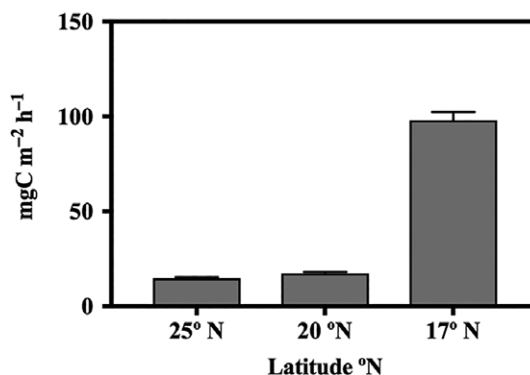


**Fig. 6.** Column-integrated primary production rates measured at three different locations along North–South Red Sea gradient.

northern and central Red Sea ( $16 \pm 1.8 \text{ mgC m}^{-2} \text{h}^{-1}$ , equating to  $\sim 165\text{--}187 \text{ mgC m}^{-2} \text{d}^{-1}$ ) (Fig. 6).

To date, primary production measurements for the Red Sea are scarce, restricted to specific areas and mostly done following the  $^{14}\text{C}$ -method (Yentsch and Wood 1961; Levanon-Spanier et al. 1979; Veldhuis et al. 1997; Qurban et al. 2014, 2017). However, our depth-integrated  $^{13}\text{C}$ -CRDS-PP rates agreed remarkably with those reported by Qurban et al. ( $16.0 \pm 5.8 \text{ mgC m}^{-2} \text{h}^{-1}$ ) for the northern Red Sea (Qurban et al. 2014). Moreover, depth integrated rates are consistent with production rates reported for other oligotrophic areas such as the Sargasso Sea ( $\sim 180\text{--}720 \text{ mgC m}^{-2} \text{d}^{-1}$ ) (Jenkins and Goldman 1985) or the Mediterranean Sea ( $95\text{--}996 \text{ mgC m}^{-2} \text{d}^{-1}$ ) (López-Sandoval et al. 2011; Moutin and Prieur 2012). These findings further support that the CRDS can be used as a reliable tool to determine phytoplankton carbon fixation rates with the  $^{13}\text{C}$ -method in low-productive waters.

### Comments and recommendations

The use of CRDS has gained increased recognition due to its high sensitivity and relatively straightforward experimental set-up. In this study, we used the commercially available CRDS unit from Picarro (G2201-isotopic analyser for  $\text{CO}_2$  and  $\text{CH}_4$ ) to develop the  $^{13}\text{C}$ -CRDS-PP method. Using solid internal standards, the attained precision for  $\delta^{13}\text{C}$  was high ( $\pm 0.13\text{‰}$ ). However, we found that the accuracy of  $\delta^{13}\text{C}$  values was sensitive to samples with a low C content. The accuracy of  $\delta^{13}\text{C}$  obtained for the reference materials containing 10–30  $\mu\text{gC}$  ranged from 3.5 $\text{‰}$  ( $\pm 0.4\text{‰}$ ) to 0.9 $\text{‰}$  ( $\pm 0.1\text{‰}$ ), whereas the accuracy for samples containing 100  $\mu\text{gC}$  (or more) improved to  $\sim 0.5\text{‰}$ . The lowest carbon content analyzed in our samples was 30  $\mu\text{gC}$ . The  $\delta^{13}\text{C}$  accuracy for this carbon concentration was  $\sim \pm 1\text{‰}$ , which represents less than 1% of the  $\delta^{13}\text{C}$  values measured in the light bottles ( $\delta^{13}\text{C}_{\text{light}}$ ). This difference in  $\delta^{13}\text{C}$  values is negligible in our primary production estimates as evidenced by the similar  $^{13}\text{C}$ -CRDS-PP results obtained from samples containing 30  $\mu\text{gC}$  and 160  $\mu\text{gC}$  (samples of different volumes).

However, traces of labeled DIC in the filters (due to incomplete removal of DIC during acidification) can significantly affect the final <sup>13</sup>C-PP estimate. For example, in the dark bottles,  $\pm 1\text{‰}$  variance in  $\delta^{13}\text{C}$  may be significant. However, because the  $\delta^{13}\text{C}_{\text{light}}$  bottles were 400–500‰, a  $\pm 1\text{‰}$  change in the  $\delta^{13}\text{C}_{\text{dark}}$  would not significantly modify <sup>13</sup>C-PP results. Furthermore, if we exclude our  $\delta^{13}\text{C}_{\text{dark}}$  values from the primary productivity calculations, <sup>13</sup>C-PP remains unaltered (Mann–Whitney test,  $U = 64$ ,  $p = 0.67$ ). Nevertheless, we recommend keeping  $\delta^{13}\text{C}_{\text{dark}}$  measurements, as they serve as a corrective factor; enrichment in  $\delta^{13}\text{C}_{\text{dark}}$  indicates that labeled DIC is still present in the filters after the acidification process.

In summary, our study shows that primary production rates derived by the <sup>13</sup>C-CRDS-PP are similar to those attained by IRMS, even in samples with low carbon content (30–50  $\mu\text{gC}$ ); thus, this laser technique is a compelling alternative to the IRMS as it is relatively much simpler to use but also cost-effective. Moreover, <sup>13</sup>C-CRDS-PP rates measured in the Red Sea agreed with expected values for an oligotrophic area, and compare to data previously reported for similar locations, but determined with the <sup>14</sup>C-radiocarbon technique.

## References

- Balch, W., M. Abbott, and R. Eppley. 1989. Remote sensing of primary production—I. A comparison of empirical and semi-analytical algorithms. *Deep-Sea Res. Part A Oceanogr. Res. Pap.* **36**: 281–295. doi:10.1016/0198-0149(89)90139-8
- Balslev-Clausen, D., T. W. Dahl, N. Saad, and M. T. Rosing. 2013. Precise and accurate  $\delta^{13}\text{C}$  analysis of rock samples using Flash Combustion–Cavity Ring Down Laser Spectroscopy. *J. Anal. At. Spectrom* **28**: 516–523. doi:10.1039/c2ja30240c
- Bass, A. M., N. C. Munksgaard, D. O’Grady, M. J. M. Williams, H. C. Bostock, S. R. Rintoul, and M. I. Bird. 2014. Continuous shipboard measurements of oceanic  $\delta^{18}\text{O}$ ,  $\delta\text{D}$  and  $\delta^{13}\text{CDIC}$  along a transect from New Zealand to Antarctica using cavity ring-down isotope spectrometry. *J. Mar. Syst.* **137**: 21–27. doi:10.1016/j.jmarsys.2014.04.003
- Becker, M., N. Andersen, B. Fiedler, P. Fietzek, A. Körtzinger, T. Steinhoff, and G. Friedrichs. 2012. Using cavity ringdown spectroscopy for continuous monitoring of  $\delta^{13}\text{C}$  ( $\text{CO}_2$ ) and  $f\text{CO}_2$  in the surface ocean. *Limnol. Oceanogr.*: Methods **10**: 752–766. doi:10.4319/lom.2012.10.752
- Behrenfeld, M. J., and P. G. Falkowski. 1997. Photosynthetic rates derived from satellite-based chlorophyll concentration. *Limnol. Oceanogr.* **42**: 1–20. doi:10.4319/lo.1997.42.1.0001
- Berden, G., R. Peeters, and G. Meijer. 2000. Cavity ring-down spectroscopy: Experimental schemes and applications. *Int. Rev. Phys. Chem.* **19**: 565–607. doi:10.1080/014423500750040627
- Crosson, E. 2008. A cavity ring-down analyzer for measuring atmospheric levels of methane, carbon dioxide, and water vapor. *Appl. Phys. B* **92**: 403–408. doi:10.1007/s00340-008-3135-y
- Crosson, E. R., and others. 2002. Stable isotope ratios using cavity ring-down spectroscopy: Determination of  $^{13}\text{C}/^{12}\text{C}$  for carbon dioxide in human breath. *Anal. Chem.* **74**: 2003–2007, doi:10.1021/ac025511d
- Garcias-Bonet, N., and C. M. Duarte. 2017. Methane production by seagrass ecosystems in the Red Sea. *Front. Mar. Sci.* **4**: 340. doi:10.3389/fmars.2017.00340
- Hansen, H. P., and F. Koroleff. 1999. Determination of nutrients, p. 159–228. *In* K. Grasshoff, K. Kremling and M. Ehrhardt [eds.], *Methods of seawater analysis*. Wiley-VCH Verlag.
- Ichimura, S., Y. Saijo, and Y. Aruga. 1962. Photosynthetic characteristics of marine phytoplankton and their ecological meaning in the chlorophyll method. *Bot. Mag. Tokyo* **75**: 212–220.
- Jenkins, W., and J. Goldman. 1985. Seasonal oxygen cycling and primary production in the Sargasso Sea. *J. Mar. Res.* **43**: 465–491. doi:10.1357/002224085788438702
- Kirsten, W. J., and G. U. Hesselius. 1983. Rapid, automatic, high capacity Dumas determination of nitrogen. *Microchem. J.* **28**: 529–547. doi:10.1016/0026-265X(83)90011-5
- Kürten, B., and others. 2016. Carbon and nitrogen stable isotope ratios of pelagic zooplankton elucidate ecohydrographic features in the oligotrophic Red Sea. *Prog. Oceanogr.* **140**: 69–90, DOI: 10.1016/j.pocean.2015.11.003
- Levanon-Spanier, I., E. Padan, and Z. Reiss. 1979. Primary production in a desert-enclosed sea—The Gulf of Elat (Aqaba), Red Sea. *Deep-Sea Res. Part A. Oceanogr. Res. Pap.* **26**: 673–685. doi:10.1016/0198-0149(79)90040-2
- López-Sandoval, D. C., A. Fernández, and E. Marañón. 2011. Dissolved and particulate primary production along a longitudinal gradient in the Mediterranean Sea. *Biogeosciences* **8**: 815–825. doi:10.5194/bg-8-815-2011
- López-Sandoval, D. C., A. Delgado-Huertas, and S. Agustí. 2018. The  $^{13}\text{C}$  method as a robust alternative to  $^{14}\text{C}$ -based measurements of primary productivity in the Mediterranean Sea. *J. Plankton Res.* **40**: 544–554. doi:10.1093/plankt/fby031
- Mousseau, L., S. Dauchez, L. Legendre, and L. Fortier. 1995. Photosynthetic carbon uptake by marine phytoplankton: Comparison of the stable ( $^{13}\text{C}$ ) and radioactive ( $^{14}\text{C}$ ) isotope methods. *J. Plankton Res.* **17**: 1449–1460. doi:10.1093/plankt/17.7.1449
- Moutin, T., and L. Prieur. 2012. Influence of anticyclonic eddies on the Biogeochemistry from the Oligotrophic to the Ultraoligotrophic Mediterranean (BOUM cruise). *Biogeosciences* **9**: 3827–3855. doi:10.5194/bg-9-3827-2012
- Nielsen, E. S. 1952. The use of radio-active carbon ( $^{14}\text{C}$ ) for measuring organic production in the sea. *ICES J. Mar. Sci.* **18**: 117–140. doi:10.1093/icesjms/18.2.117

- Picarro. 2009. WS-CRDS for isotopes-cost of measurement comparison with IRMS for liquid water. Picarro Inc.
- Qurban, M. A., A. C. Balala, S. Kumar, P. S. Bhavya, and M. Wafar. 2014. Primary production in the northern Red Sea. *J. Mar. Syst.* **132**: 75–82. doi:[10.1016/j.jmarsys.2014.01.006](https://doi.org/10.1016/j.jmarsys.2014.01.006)
- Qurban, M. A., M. Wafar, R. Jyothibabu, and K. P. Manikandan. 2017. Patterns of primary production in the Red Sea. *J. Mar. Syst.* **169**: 87–98. doi:[10.1016/j.jmarsys.2016.12.008](https://doi.org/10.1016/j.jmarsys.2016.12.008)
- Raitsos, D. E., Y. Pradhan, R. J. Brewin, G. Stenichkov, and I. Hoteit. 2013. Remote sensing the phytoplankton seasonal succession of the Red Sea. *PLoS One* **8**: e64909. doi:[10.1371/journal.pone.0064909](https://doi.org/10.1371/journal.pone.0064909)
- Regaudie-de-Gioux, A., S. Lasternas, S. Agustí, and C. M. Duarte. 2014. Comparing marine primary production estimates through different methods and development of conversion equations. *Front. Mar. Sci.* **1**: 19. doi:[10.3389/fmars.2014.00019](https://doi.org/10.3389/fmars.2014.00019)
- Sakamoto, M., and others. 1984. Joint field experiments for comparisons of measuring methods of photosynthetic production. *J. Plankton Res.* **6**: 365–383, doi:[10.1093/plankt/6.2.365](https://doi.org/10.1093/plankt/6.2.365)
- Slawyk, G., Y. Collos, and J. C. Auclair. 1977. The use of the <sup>13</sup>C and <sup>15</sup>N isotopes for the simultaneous measurement of carbon and nitrogen turnover rates in marine phytoplankton. *Limnol. Oceanogr.* **22**: 925–932. doi:[10.4319/lo.1977.22.5.0925](https://doi.org/10.4319/lo.1977.22.5.0925)
- Slawyk, G., M. Minas, Y. Collos, L. Legendre, and S. Roy. 1984. Comparison of radioactive and stable isotope tracer techniques for measuring photosynthesis: <sup>13</sup>C and <sup>14</sup>C uptake by marine phytoplankton. *J. Plankton Res.* **6**: 249–257. doi:[10.1093/plankt/6.2.249](https://doi.org/10.1093/plankt/6.2.249)
- Smith, R., R. Eppley, and K. Baker. 1982. Correlation of primary production as measured aboard ship in southern California coastal waters and as estimated from satellite chlorophyll images. *Mar. Biol.* **66**: 281–288. doi:[10.1007/BF00397033](https://doi.org/10.1007/BF00397033)
- Veldhuis, M. J., G. W. Kraay, J. D. Van Bleijswijk, and M. A. Baars. 1997. Seasonal and spatial variability in phytoplankton biomass, productivity and growth in the northwestern Indian Ocean: The southwest and northeast monsoon, 1992–1993. *Deep-Sea Res. I Oceanogr. Res. Pap.* **44**: 425–449. doi:[10.1016/S0967-0637\(96\)00116-1](https://doi.org/10.1016/S0967-0637(96)00116-1)
- Yentsch, C. S., and L. Wood. 1961. Measurements of primary production in the Red Sea, Gulf of Aden and Indian Ocean. Wood Hole Oceanographic Institution: Ref 61–66, Appendix 68:66.
- Zarokanellos, N., V. P. Papadopoulos, S. Sofianos, and B. Jones. 2017. Physical and biological characteristics of the winter-summer transition in the Central Red Sea. *J. Geophys. Res. Oceans* **122**: 6355–6370. doi:[10.1002/2017JC012882](https://doi.org/10.1002/2017JC012882)

### Acknowledgments

The research reported in this publication was supported by funding from King Abdullah University of Science and Technology (KAUST), under award number BAS/1/1071-01-10 assigned to CMD, BAS/1/1072-01-01 assigned to SA, and FCC/1/1973-21-01 assigned to the Red Sea Research Center. We also thank to the anonymous referees for their helpful and valuable comments and suggestions to improve our manuscript.

### Conflict of Interest

None declared.

*Submitted 16 May 2018*

*Revised 13 December 2018*

*Accepted 18 December 2018*

*Associate editor: Tammi Richardson*